A novel electro-stimulated drug delivery system based on PLLA composites exploiting the multiple functions of graphite nanoplatelets

ACS APPLIED MATERIALS & INTERFACES

Research Article

www.acsami.org

A Novel Electrostimulated Drug Delivery System Based on PLLA Composites Exploiting the Multiple Functions of Graphite Nanoplatelets

Lorenza Gardella,[†] Samuele Colonna,[‡] Alberto Fina,[‡] and Orietta Monticelli*[,†]

[†]Dipartimento di Chimica e Chimica Industriale, Università di Genova, Via Dodecaneso, 31, 16146 Genova, Italy

[‡]Dipartimento di Scienza Applicata e Tecnologia, Politecnico di Torino-sede di Alessandria, viale Teresa Michel, 5, 15121 Alessandria, Italy

Supporting Information

ABSTRACT: A novel drug delivery system based on poly(L-lactide) (PLLA), graphite, and porphyrin was developed. In particular, 5,10,15,20-tetrakis(4-hydroxyphenyl)porphyrin (THPP) was chosen because, besides its potential as codispersing agent of graphite, it is a pharmacologically active molecule. Graphite nanoplatelets, homogeneously dispersed in both the neat PLLA and the PLLA/porphyrin films, which were prepared by solution casting, turned out to improve the crystallinity of the polymer. Moreover, IR measurements demonstrated that unlike PLLA/porphyrin film, where the porphyrin was prone to aggregate causing variable concentration throughout the sample, the system containing also GNP was characterized by a homogeneous dispersion of the above molecule. The effect of graphite nanoplatelets on the thermal stabilization, electrical conductivity, and improvement of mechanical properties of the polymer resulted to be increased by the addition of the porphyrin to the system, thus demonstrating the role of the molecule in ameliorating the filler dispersion in PLLA. The porphyrin release from the composite film, occurring both naturally and with the application of an electrical field, was measured using an UV−vis spectrophotometer. Indeed, voltage application turned out to improve significantly the kinetic of drug release. The biocompatibility of the polymer matrix as well as the mechanical and thermal properties of the composite together with its electrical response makes the developed material extremely promising in biological applications, particularly in the drug delivery field.

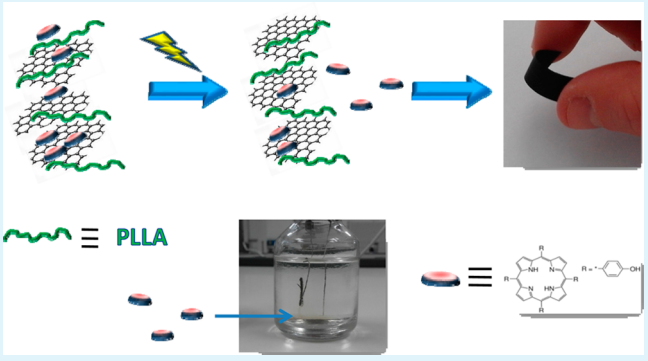

KEYWORDS: *drug release, PLLA, composites, graphite, electrical conductivity, porphyrin*

INTRODUCTION

The combination of carbon-based particles/nanoparticles such as graphite/graphene-related materials with polymers has been widely investigated[1,2] because of the improved properties of the resulting composites/nanocomposites as well as for the features, such as electrical[3,4] and thermal conductivity,[5] conferred to the polymer matrix. Among the different applications which were envisaged for such materials, so far, a limited number of studies have considered their applicability in the biomedical field. Indeed, neat graphene-related materials have been widely explored for drug delivery systems because they exhibit important qualities such as low cost, facile fabrication and modification, high surface area, biocompatibility, and purity.[6−8] For these reasons, since Dai's pioneering work,[9] first demonstrating that poly(ethylene glycol) (PEG)-functionalized graphene oxide (GO) can be used as a drug carrier, carbon materials and nanomaterials have been extensively explored for the loading of different therapeutics, including anticancer drugs,[8−12] DNA,[13,14] and genes.[15] Clearly, the combination of the carbon material/drug system with a biocompatible/bioabsorbable polymer represents a relevant advantage in the development of systems where the drug release occurs by applying a structural material, such as in the tissue engineering.[16] In this case, besides acting as a drug carrier thus facilitating its homogeneous dispersion in the polymer matrix, the filler can confer electrical conductivity to the material, producing electrically responsive/controlled drug delivery system. Indeed, the above material may offer unique advantages for providing the on-demand release of drugs to reach a rapid and efficacious therapy by powder supply. Moreover, when combined with a sensor, feedback and remote control of the device outside the body become possible. In the field of stimulus-responsive materials for the drug release, inherently conductive polymers are commonly applied, such as polypyrrole,[17,18] polyaniline,[19] polythiophene derivatives,[20] etc. Despite the wide applicability of these polymers, some specific

Received: July 18, 2016
Accepted: September 1, 2016
Published: September 1, 2016

DOI: 10.1021/acsami.6b08808
ACS Appl. Mater. Interfaces 2016, 8, 24909−24917

issues need to be considered, that is, mainly their poor mechanical properties, which compel to combine and/or deposit them on other polymers and the not always easy dispersion of the drug.[21] On this basis, biocompatible polymers, characterized by good mechanical properties and which can be made conductive by the inclusion of proper additives, might represent a valid alternative to the above systems in the development of structural material to be used in the controlled drug delivery.

With this in mind, in this work a novel material was developed, consisting of a biocompatible polymer, that is, poly(L-lactide) (PLLA), in which the dispersed/exfoliated graphite nanoplatelets can both act as a drug carrier and make the system conductive. Indeed, recently, PLA-based materials containing carbon filler/nanofiller have been widely studied as they show improved crystallization rate[22−24] as well as mechanical and gas barrier properties[25] with comparison to the neat polymer matrix. In general, the preparation of PLA/graphene-related materials was carried out either by applying the solution-mixing approach[26,27] or by using melt mixing.[28] The former method implies the preliminary dispersion of the layered carbon filler in a solvent able to promote exfoliation and to disperse the graphene layers as well as to solubilize the polymer. Furthermore, in order to enhance the compatibility with the polymer matrix, graphene oxide was commonly exploited. The use of GO requires the oxidation of graphite, typically performed by using strong acids and oxidating agents,[29] thus achieving the extensive modification of the carbon atoms hybridization and hence to restore sp^2-based graphene layers, which is fundamental for the electrical and thermal conductivity, subsequent reduction of GO has to be performed.[30] Clearly, the application of methods directly starting from graphite, such as the simple and effective liquid-phase exfoliation, is highly desirable. In particular, in the above approach, the key parameter for suitable solvents is that the solvent−graphene interactions must be at least comparable to those existing between the stacked graphene layers in graphite.[31] Also, the use of small organic molecules, such as surfactants, can promote the exfoliation of graphite into graphene, in particular when such molecules have a high energy of adsorption on the basal plane of graphene, which energy must be higher than the one of the solvent molecule interacting with graphene.[32,33] Although not widely applied as other surfactants, such as pyrene-based molecules,[34] also porphyrins were found to interact with various carbon materials, such as graphite,[35,36] fullerenes,[37] and carbon nanotubes (CNTs),[38] through π stacking that takes place between their electron-abundant aromatic cores and conjugated surfaces of the carbon materials. Indeed, Geng et al.[36] used 5,10,15,20-tetraphenyl-(4,11-acetylthioundecyloxyphenyl)-porphyrin (TATPP), which, strongly interacting with the graphite surface, proved capable to produce monolayered graphene sheets of high quality in the TATPP-assisted exfoliation of graphite. Besides considering the specific interactions of such molecules with the surface of graphite, it is relevant to underline that some kinds of porphyrin are pharmacological active species, which were applied in the cancer treatment and for their antimicrobical properties.[39−41] In particular, 5,10,15,20-tetrakis(4-hydroxyphenyl)porphyrin (THPP), the object of the present study, which can be considered a model drug, was recently used as antibacterial.[40]

To summarize, this work deals with the development of novel composite systems based on PLLA, where the graphite nanoplatelets can perform multiple roles (Figure 1): (i) interact with the porphyrin, thus promoting its dispersion in the

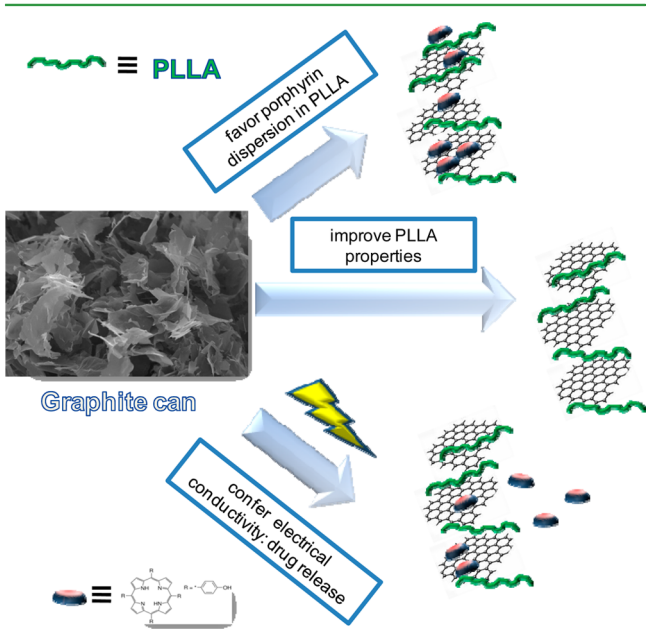

Figure 1. Scheme of the possible functions of graphite in the composite system.

polymer matrix, (ii) improve the properties of the polymer, and (iii) confer electrical conductivity to the system, which feature can be used to tune the drug release. Furthermore, as already hinted, the pharmacologically active porphyrin could, in turn, favor the dispersion/exfoliation of graphite. Indeed, the work was first developed by verifying the effect of the chosen porphyrin on the exfoliation of graphite in a solvent, namely dimethylformamide (DMF), capable also of solubilizing PLLA and on the stabilization of such dispersion in time. The composite systems, prepared by solution casting, were characterized in terms of morphology as well as thermal, mechanical, and electrical properties not only to verify the effect of the filler on the above features but also because, in the development of the structural stimulus-responsive material, it is essential to know deeply the characteristics of the matrix where the drug is dispersed and it is released. The porphyrin released from the composite film, both occurring naturally and with the application of an electrical field, was quantitatively measured.

EXPERIMENTAL SECTION

Materials. Poly(L-lactide) (PLLA) is a commercial product from Nature Works Co. Ltd. U.S.A. (2002D, M_n = 100 000 g/mol) with a residual monomer content less than 0.3 mass %. Graphite nanoplatelets, A12 grade from Graphene Supermarket (USA), with particle size distribution from 2 to 8 μm (Figure S1), were used as received.

5,10,15,20-Tetrakis(4-hydroxyphenyl)porphyrin (THPP) was purchased from Sigma-Aldrich as crystalline powders and used as received (Figure S2). Anhydrous dimethylformamide (99.8%), phospate-buffered saline (PBS, pH = 7), and acetone were purchased from Sigma-Aldrich and used without further purification.

Preparation of the Composite Systems. For the composite film preparation (named PLLA_G), an appropriate amount of the filler was first dispersed in DMF at room temperature by sonication in a sonic bath (Model Ney Ultrasonic) at 40 kHz for 1 h. Before accomplishing the film preparation, the polymer was dried overnight at 40 °C. The dispersion was mixed with a solution of PLLA dissolved in DMF at 80 °C, cast onto a glass Petri dish, and dried under vacuum for 24 h at 80

DOI: 10.1021/acsami.6b08808
ACS Appl. Mater. Interfaces 2016, 8, 24909−24917

°C to completely remove the solvent. In the case of the system based on porphyrin (named PLLA_G_p), the latter was added in the DMF/graphite dispersion. The final concentrations of graphite and porphyrin in the film were 2 and 0.4 wt % with respect to PLLA, respectively. For the sake of comparison, films based on neat PLLA (named PLLA) and PLLA/porphyrin (named PLLA_p) were prepared by applying the same method and equal polymer/porphyrin ratio as above.

In order to evaluate the capacity of DMF and of the system DMF/porphyrin to disperse/exfoliate the filler, 35 mg of graphite was dispersed by sonication for 1 h in 5 mL of DMF or in the same amount of solvent containing 7 mg of porphyrin. The resultant dispersion was then centrifuged using a Hettich Mikro 22R centrifuge for 30 min at 8000 rpm. The precipitate was separate from the solvent, and the dispersion was then centrifuged again.

Characterization. A Zeiss Supra 40 VP field emission scanning electron microscope (FE-SEM) equipped with a backscattered electron detector was used to examine the composite morphologies. The specimens were submerged in liquid nitrogen for 30 min and fractured cryogenically. All samples were thinly sputter-coated with carbon using a Polaron E5100 sputter-coater. The above FE-SEM was also applied to evaluate the graphite morphology in the solvent by depositing a drop of the dispersion on a sample holder typically used for the transmission electron microscopy (TEM) measurements.

Thermal gravimetrical analysis (TGA) was performed with a Mettler-Toledo TGA 1 thermogravimetric analyzer, under a flow of nitrogen of 80 mL/min.

FTIR spectra were recorded on a Bruker IFS66 spectrometer in the spectral range 400−4000 cm^{-1}.

Differential scanning calorimetric (DSC) analysis was performed under a continuous nitrogen purge on a Mettler calorimetric apparatus (model DSC1 STAR^e system). Both calibrations of heat flow and temperature were based on a run in which one standard sample (indium) was heated through its melting point. The samples, having a mass between 2.5 and 6 mg, were heated from room temperature to 200 °C, then cooled down to room temperature, and finally heated to 200 °C again. A scanning rate of 10 °C/min was used on both heating and cooling. The reported T_g (glass transition temperature) and T_m (melting temperature) values were defined as the midpoints of the sigmoidal curve and maxima of the endotherms, respectively.

The tensile properties were determined at room temperature by an Instron Mechanical Tester (Instron 5565) at a crosshead speed of 5 mm/min using rectangular specimens with dimension of 10 × 25 × 0.5 mm. The reported property values represent an average of the results for tests run on six specimens along with their experimental deviation.

Electrical resistivity (volumetric) was evaluated with a homemade apparatus on 0.5 mm thick films prepared by casting as described above and cut in stripes.

The apparatus for the measurement is composed by a tension and direct current regulated power supply (PR18-1.2A of Kenwood, Japan), a numeral table multimeter (8845A of Fluke, Everette/USA) equipped with a digital filter in order to reduce the noise of the measure, a palm-sized multimeter (87 V of Fluke, Everette/USA), two electrodes connected at the ends of the specimen, and knife-shaped electrodes placed on the film at a distance of 12.5 mm between these. With a current imposed on the film by the terminal electrodes, the voltage drop between knife electrodes is measured to calculate the resistance and resistivity, given the cross section and distance between knife electrodes.

Porphyrin Release Test. For the porphyrin release test, a dried PLLA/graphite/porphyrin film (PLLA_G_p), measuring 1 cm (length) × 1 cm (wide) × 0.1 cm (thick), was placed in container containing 15 mL of a 1/1 v/v acetone/PBS mixture. The film was connected to a platium electrode while the other platinum electrode was placed at a distance of 1 cm. The film was exposed to an electric voltage, generated by a dc power source, of 2 V. In another container, a film characterized by the same dimension was kept in contact with the same solution without any electrostimulation. The amount of porphyrin released was measured using a UV−vis spectrophotometer (Varian Cary 100 spectrometer) at various time intervals.

RESULTS AND DISCUSSION

In this work, the effect of porphyrin on the dispersion/exfoliation as well as on the stabilization of graphite in DMF has been initially investigated. Indeed, the above solvent was chosen because, as reported by Hernandez et al.,[43] it is capable of promoting the graphite exfoliation, it being characterized by a surface energy comparable to that of graphene. The photographs of the systems DMF/GNP and DMF/GNP/porphyrin, which underwent a process of sonication and centrifugation, are shown in Figure 2.

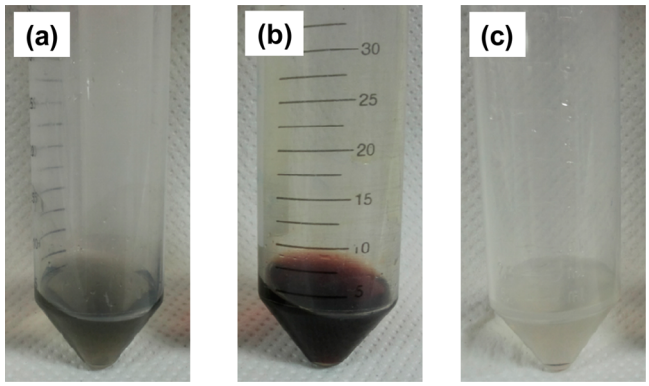

Figure 2. Photographs of GNP dispersions, after sonication and centrifugation treatment, in (a) DMF (fresh suspension), (b) DMF/porphyrin (one month aged suspension), and (c) DMF (one month aged suspension).

The former solution appears to be slightly gray (Figure 2a) while the second one, due to the color of the solubilized porphyrin, is dark (Figure 2b), thus preventing a visual comparison between the color of the two systems. It is worth underlining that the dispersion of the filler in DMF turned out to change with time: when comparing a fresh graphite-based suspension with a one-month-old system, it is possible to notice in the latter a residue and a reduction in the light absorbance, i.e., a reduction in concentration of GNP suspension (Figure 2c). This phenomenon demonstrates the scarce capacity of the solvent alone to kinetically stabilize the graphite nanoplatelets dispersion. As such, in order to evidence the effect of the porphyrin, if any, one-month-aged dispersions were studied by means of SEM by depositing a drop of the suspension on a sample holder. Unlike the dispersion in neat DMF, where graphite aggregates were almost absent, the sample containing the porphyrin was characterized by an elevated concentration of particles with an average dimension of 5 μm and a limited numbers of layers (Figure 3a). Clearly, this difference may be attributed to the specific interactions occurring between the porphyrin and the surface of graphite, which, as already reported, can from one part improve the exfoliation of the filler in the solvent and from the other affect the stabilization of the dispersion, the organic molecule acting as a kind of compatibilizer between graphite and the solvent. These interactions were investigated also by using FT-IR measurements.

Indeed, Figure 4 compares the IR spectra of the neat GNP and porphyrin with that of GNP which underwent a sonication treatment in a solution containing porphyrin and a subsequent

DOI: 10.1021/acsami.6b08808
ACS Appl. Mater. Interfaces 2016, 8, 24909−24917

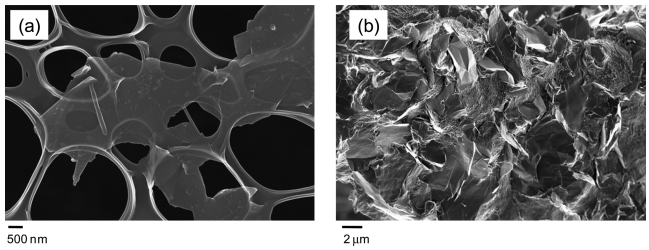

Figure 3. FE-SEM micrographs of (a) the graphite nanoplatelets dispersed by sonication in DMF/porphyrin and (b) PLLA_G_p.

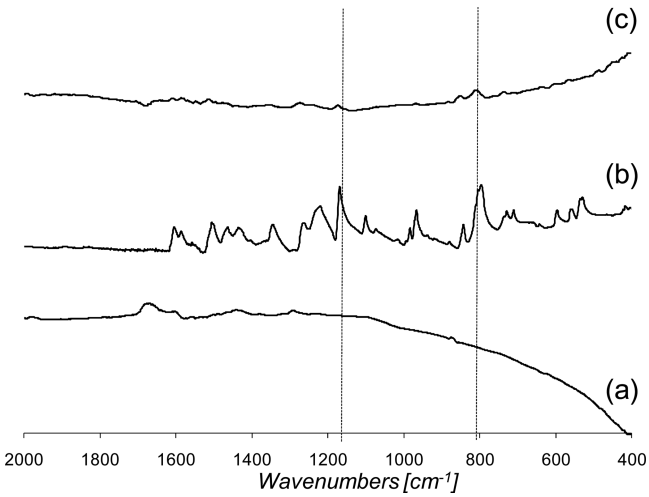

Figure 4. FT-IR spectra of (a) neat GNP, (b) neat porphyrin, and (c) residue of GNP after a sonication treatment with porphyrin and centrifugation.

centrifugation. The deposit of GNP after the centrifugation was analyzed by IR. In the latter spectrum, obtained by subtracting the spectrum of graphite, the most intense peaks of porphyrin at 790 and 1166 cm^{-1} are visible. This finding is a proof of the interaction porphyrin−graphite, which causes the anchoring of the porphyrin to the surface of graphite. It is worth underlining that this aspect might be of particular relevance in the development of the composite films, as the above interactions might potentially promote the dispersion of the porphyrin in the polymer matrix.

Composite films were prepared by mixing at 80 °C a polymer solution in DMF with that obtained by dispersing/exfoliating the graphite in the same solvent through a sonication treatment. It is important to underline that in the case of the film preparation the centrifugation was not applied in order to maintain the GNP concentration of solution in the film. In Figure 3b, SEM micrograph of the sample PLLA_G_p is shown. It is clear, in the fragile fracture of cross section of the sample, the presence of homogeneously distributed aggregates which are characterized by lateral dimensions in the range of a few micrometers, similar to that of the GNP as received. The dimensional stability of the filler demonstrates that the procedure applied for the preparation of the composite systems is suitable. The morphology of the sample based on graphite (PLLA_G) is very similar to that found for the system containing the porphyrin (Figure S3); that is, the microscope characterization does not evidence significant differences between the dispersion of graphite in the two samples. Nevertheless, it is clear that the material properties, which will be described in the following, may be correlated to the degree of dispersion/exfoliation of the filler in the two investigated systems. In this work, not only the influence of the porphyrin on the graphite dispersion was investigated but also the effect of the filler on the distribution of the above molecule in the polymer matrix. A PLLA/porphyrin film (PLLA_p) was prepared by applying the same conditions and polymer/porphyrin ratio used for the preparation the composite systems.

This film, whose photograph is reported in Figure 5A, shows an uneven color, and unlike the PLLA/graphite/porphyrin system (Figure 5B), it is characterized by a significant surface roughness.

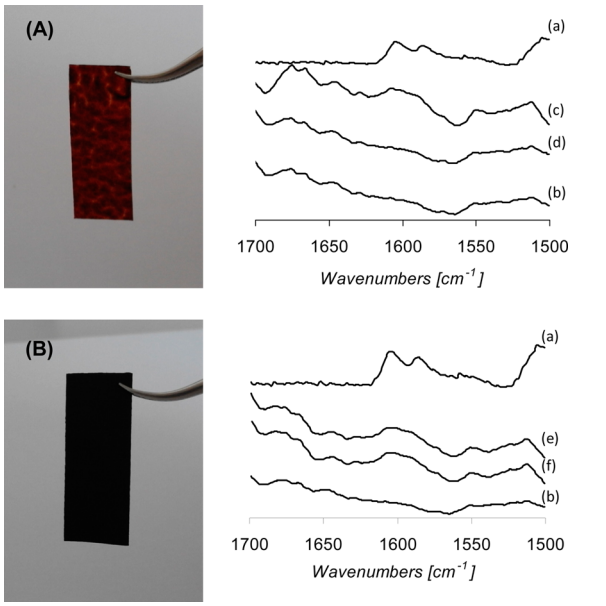

Figure 5. Photographs of (A) PLLA_p and (B) PLLA_G_p films; IR spectra of (a) neat porphyrin, (b) neat PLLA, (c) PLLA_p film (area 1), (d) PLLA_p film (area 2), (e) PLLA_G_p film (area 1), and (f) PLLA_G_p (area 2).

FT-IR measurements allowed to quantify the concentration of the porphyrin in different areas of the films. Figure 5 compares the IR spectra of the PLLA/porphyrin and PLLA/graphite/porphyrin films, which were acquired by analyzing different areas of the samples. In particular, the region between 1700 and 1500 cm^{-1} was analyzed since, in this interval of wavenumbers, no peaks are present for PLLA, but there is an absorption band of porphyrin around 1600 cm^{-1}, assigned to the bending of NH groups. In the case of the film PLLA/porphyrin/graphite, the bands of the three normalized spectra are characterized by the same absorption intensities, while those of the PLLA/porphyrin film are different. This behavior can be attributed to the different content of the porphyrin in the analyzed areas of the film, thus confirming the inhomogeneous composition of the system containing the sole porphyrin and the role of the filler in ameliorating its dispersion in the polymer matrix.

The thermal properties of PLLA_G and PLLA_G_p were studied and compared with those of neat PLLA. Figure 6 shows DSC traces of PLLA and of the samples PLLA_G and PLLA_G_p, while thermal data are summarized in Table 1. By comparing the behavior of PLLA with that of the sample containing graphite, PLLA_G, it is evident that the presence of the filler increases significantly ΔH_m and ΔH_{cc}. On the basis of

DOI: 10.1021/acsami.6b08808
ACS Appl. Mater. Interfaces 2016, 8, 24909−24917

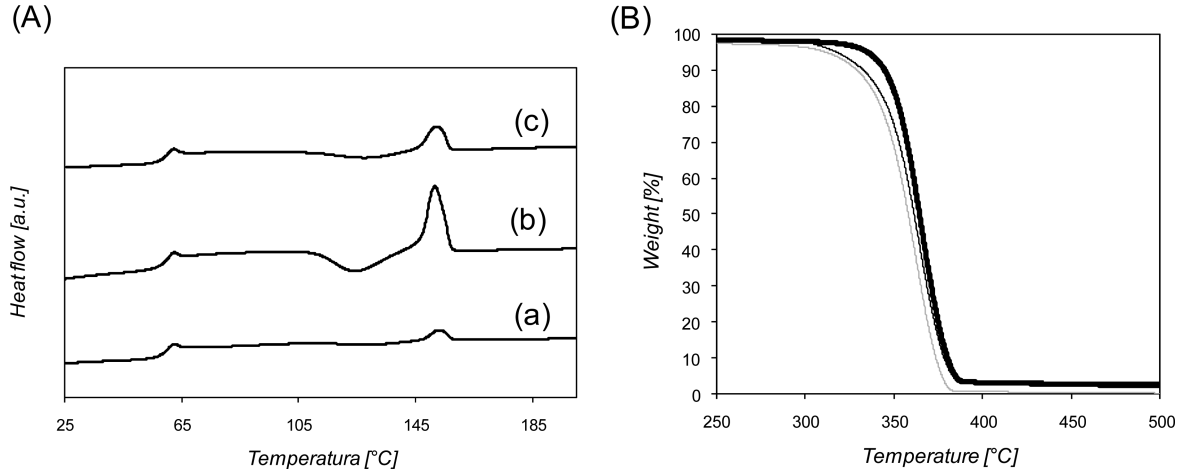

Figure 6. (A) DSC traces (endo up ↑) of (a) PLLA, (b) PLLA_G, and (c) PLLA_G_p. (B) TGA curves: (gray line) PLLA, (thin line) PLLA_G, and (thick line) PLLA_G_p.

Table 1. Properties of Neat PLLA and of the Prepared Materials Based on Graphite

sample	T_g [°C]	T_{cc} [°C]	ΔH_{cc} [J g^{-1}]	T_m [°C]	ΔH_m [J g^{-1}]	T_{onset} [°C]	T_{max} [°C]	resistivity [Ω m]
PLLA	61	130	3	153	3	311	364	~10^{15}
PLLA_G	61	124	20	152	21	317	367	4.5×10^{-2}
PLLA_G_p	60	129	8	152	8	335	368	1.7×10^{-2}

the heat of fusion of 100% crystalline PLLA, that is, 93 J g^{-1},[44] the degree of crystallinity (W_c) can be estimated to be around 3% and 21% for neat PLLA and PLLA_G, respectively. In addition, the difference of T_{cc} between neat PLLA and the composite system is ca. 7 °C. These findings highlight the capacity of GNP to improve the crystallizability of the polymer matrix already at loading as low as 2 wt % with respect to PLLA. As mentioned above, the specific influence of graphite/graphene on the crystallization of PLA was previously reported. In particular, Xu et al.[45] demonstrated the possibility to apply graphene nanosheets as efficient heterogeneous nucleating agent for PLA. More recently, a different behavior of the above nanofiller was found by Wu et al.,[22] who verified that graphene nanosheets act as inert fillers during cold crystallization and as heterogeneous nucleating agents only during melt crystallization. Similar observations were reported also by Su and He.[46] A different trend of T_{cc}, similar to that reported in our work, that is, a decrease of T_{cc} in the graphene-based composites with respect to the neat polymer matrix, was found in systems PLA/GO, and such a phenomenon was ascribed to the nucleating effect of the filler.[47] It can be hypothesized that the differences found in the described systems are related to both the different grade of PLAs employed, such as the diverse D/L ratio, and to the different filler form and dispersion. It is of utmost relevance to underline that in most of the mentioned works GO was used, as this nanofiller is more compatible and easily dispersible in the polymer matrix. Although the application of GO helps to improve the final material properties, the preparation of GO by preliminary treatment of graphite is generally time-consuming and costly and needs subsequent reduction to restore the electrical conductivity. Conversely, in our work it was demonstrated that starting from graphite, by simply coupling a suitable solvent with a sonication process, it is possible to obtain a system where the disperse/exfoliate graphite is capable of enhancing the final properties of the material even by using a limited filler concentration, i.e., 2 wt % with respect to PLLA.

Furthermore, it is worth underling an aspect which was not well documented in the literature but important in the development of composites based on graphite, that is, that the peculiar features of the fillers, such as the lateral dimensions of the layers, play a key role in determining the final properties of the composites. Indeed, the type of graphite used in this work was selected as the optimal after having studied the features, in terms of dispersion and conductivity, of composites based on graphite nanoplatelets characterized by different aspect ratios. Although the different types of GNP did not affect the film formation and its mechanical stability, as reported in the Table S1, the lateral dimension of the filler turned out to strongly influence the material conductivity. Indeed, among the three used GNP, only grade A12 from Graphene Supermarket was found to confer electrical conductivity to the material, in the range of 10^1 S/m.

Thermal data reported in Figure 6A and Table 1 reveal that the ΔH_{cc} and ΔH_m of the sample containing porphyrin and graphite (PLA_G_p) are lower than that of PLA_G. Accordingly, as the presence of the porphyrin in the system seems to inhibit the nucleating effect of graphite, it is possible to hypothesize that the interactions between the above molecule and the surface of graphite, which occur through π-stacking, modify the interplay between the polymer and the filler, thus limiting the effect of the latter in promoting polymer structuring into crystal domains. Nevertheless, it is important to underline that also in the sample based on porphyrin, the capacity of the graphite to increase the polymer crystallinity is not completely annulled, as the ΔH_{cc} and ΔH_m of the composite system PLLA/graphite/porphyrin turn out to be 3 times higher than those of neat PLLA.

The study of the influence of graphite on PLLA thermal properties was completed by carrying out also thermal gravimetric analysis (TGA). Figure 6B compares TGA curves of the neat PLLA with those of the systems containing graphite (PLLA_G and PLLA_G_p). As already reported for other

DOI: 10.1021/acsami.6b08808
ACS Appl. Mater. Interfaces 2016, 8, 24909−24917

PLA-based materials,[48] the thermal decomposition of all the analyzed samples was found to occur in one step in the temperature range between ca. 300 and 400 °C. The presence of graphite is found to slightly affect the onset degradation temperature (T_{onset}), T_{onset} of PLLA being 311 °C and that of the sample containing graphite (PLLA_G) 317 °C (Table 1), while the temperature corresponding to the maximum weight loss rate (T_{max}) does not change significantly. On the other hand, in the system containing the porphyrin (PLLA_G_p) the increase of T_{onset} with respect to that of the neat PLLA is more evident, it being ca. 24 °C. In general, the enhancement of thermal stability in the system PLA/graphite (graphene), already reported in the literature,[22,45,46] was related to the high surface area as well as to the lamellar structure of the filler which, thanks to these peculiar features, acts as a barrier for the diffusion of volatile products produced during the material decomposition. On this basis, it is possible to hypothesize that the amelioration of the dispersion/exfoliation of graphite, caused by the addition of the porphyrin, enhances the GNP effect on the thermal degradation of the polymer matrix. Furthermore, another aspect, which, in our system, might influence the decomposition of PLLA is the modification of the nature of the graphite surface, which being covered with the porphyrin could exhibit different types of interactions with the molecules produced by the decomposition process.

The effect of GNP on the electrical properties of the materials was studied by comparing the volume resistivity of the neat PLLA with those of the two composite samples (Table 1). Indeed, PLLA is electrically insulating, it showing a very high resistivity, in the range of 10^{15} Ω m,[49] while the composites containing graphite are characterized by a much lower resistivity. It is worth underlining that PLA carbon-based composites, such as PLA/expanded graphite,[50] PLA/carbon black,[51] and PLA/GO,[49] with similar filler loading, exhibit a resistivity of ca. 10^4 Ω m. In some of these systems, the reduction of GO was found to reduce the resistivity up to ca. 45 × 10^{-2} Ω m.[49] The much higher conductivity of our composites with respect to the systems described in the literature might be related, as already reported, to the better exfoliation/dispersion of GNP. In particular, in our case, it is possible to hypothesize that the aspect ratio of the graphite layers is high enough for the formation of the conducting network at the loading used. Moreover, by comparing the behavior of the two samples PLLA_G and PLLA_G_p, it is evident that the presence of porphyrin in the system seems to slightly increase the material conductivity. On the basis of the above considerations, also this phenomenon can be ascribed to the influence of porphyrin on the dispersion of the filler inside the polymer matrix.

The prepared films were also characterized by mechanical tests, and the results are given in Table 2. PLLA is well-known to be a glassy polymer at room temperature,[52] it showing a relatively high modulus (1200 MPa) associated with a low deformation at break, namely about 7%. On the other hand, the graphite dispersion in the polymer matrix increases the Young's modulus (E), which passes from 1400 MPa for the neat PLLA to 2200 MPa in the case of the composite PLLA_G. These results demonstrate a reinforcing effect of the filler, which already at low concentration (2 wt %) is able to increase the modulus of about 60%. A further increase of E was found in the film containing the porphyrin (PLLA_G_p), which results to be characterized by a modulus of 2600 MPa. Conversely, the elongation at break was found not to change in the composite systems with compared to the neat PLLA film. Indeed, the reinforcing effect of graphite/graphene, reported in the literature for both PLLA and for other polymer matrices, was related to the degree of the filler dispersion in the polymer.[53] In particular, it was demonstrated that by increasing the filler concentration, the modulus tends to decrease because of the worsening of the graphite dispersion.[53] On this basis, it is possible to correlate the increase of the Young's modulus in the sample containing the porphyrin with the improvement of graphite dispersion/exfoliation in the polymer matrix.

Table 2. Mechanical Measurements Results

sample	E [MPa]	ε_{break} [%]	σ_{break} [MPa]
PLLA	1400 ± 40	4 ± 1	30 ± 4
PLLA_G	2200 ± 40	4 ± 1	31 ± 2
PLLA_G_p	2600 ± 30	5 ± 1	32 ± 4

As previously mentioned, in the prepared system, the porphyrin was used not only as a codispersing agent of graphite but, most importantly, as a model drug. The kinetic of its release from the system PLLA/graphite whose biocompatibility, and therefore applicability in the medical field, was recently demonstrated in the literature.[54]

Indeed, the possibility of incorporating the carrier/drug system in a biocompatible and bioabsorbable polymeric matrix represents a significant advantage for the development of structural material to be used in the controlled drug delivery.

UV measurements allowed to follow the concentration of the porphyrin in a solution, made of a 1/1 v/v mixture of acetone and PBS, in which the composite film PLLA_G_p was dipped, and to study the kinetics of release of the molecule, occurring both naturally and upon electrical stimulation at a constant voltage of 2 V. In Figure 7a, the ratio between the amount of the released porphyrin and that contained in the film is given as a function of time, when natural or electrically stimulated release is carried out. It is important to underline that the release from PLLA/porphyrin film was not analyzed since, as previously reported, the drug is extremely aggregated at the macroscale and its concentration varies from one zone to another in the sample, thus leading to irreproducible release kinetic. It is evident from Figure 7a that the kinetic of release from composite film PLLA_G_p, with the application of a negative potential to the film, is significantly accelerated as compared to the natural release.

In particular, it was found that the kinetics of release follow the first order in both cases, but the rate constant is greater in the case of the application of the electric field to the film, it increasing from 2.32 × 10^{-5} to 4.22 × 10^{-5} s^{-1}, i.e., an almost double release rate. Furthermore, unlike the natural release test (Figure 7b), it is well visible in the film connected to the electrodes, the release of the drug, which is characterized by an orange-red coloration, already after 10 min from the beginning of the experiments (Figure 7c,d). A possible explanation of the observed electrostimulation effect can be proposed based on previous literature report,[55] in terms of change in graphene morphology, which was indeed reported to occur during the electrical stimuli. The distortion of graphite layers and/or temporary variations of surface charges would decrease the molecular interactions with porphyrin, thus increasing its release when the film underwent electrical stimuli (Figure 7f).

It is relevant to underline that in the literature there are very few examples of composites based on carbon filler/nanofiller,

DOI: 10.1021/acsami.6b08808
ACS Appl. Mater. Interfaces 2016, 8, 24909−24917

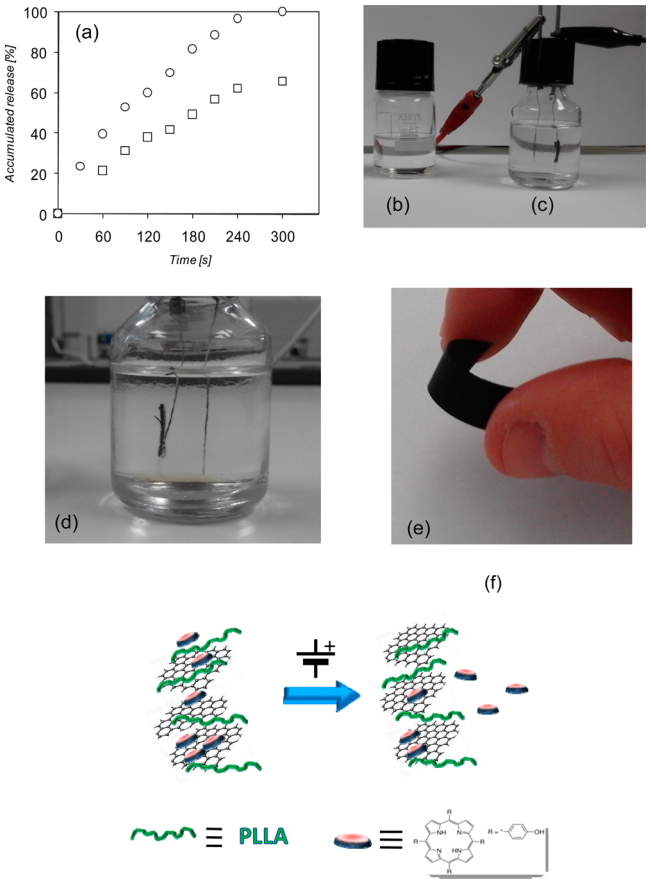

Figure 7. (a) Accumulated release as a function of time (○, electrical stimulated release; □, natural release), (b) photo of PLLA_G_p film in contact with a 1/1 v/v acetone/PBS mixture, after 10 min from the beginning of the experiment, (c) photo of PLLA_G_p film in contact with with a 1/1 v/v acetone/PBS mixture and exposed to an electric voltage, after 10 min from the beginning of the experiment, (d) detail of the latter film (a slight orange-red coloration can be appreciated below the film), (e) PLLA_G_p film after drug delivery test, and (f) scheme of the drug release in the PLLA_G_p film by electrical stimulation.

whose conductivity was exploited to stimulate the release of drugs and most of the developed materials are based on hydrogel and GO.[55−57] In particular, Liu et al.[55] studied electromodulated release of lidocaine hydrochloride from reduced GO in a poly(vinyl alcohol) (PVA) hydrogel. Although it was demonstrated that the above hydrogel displayed a faster response to electrostimulation, high voltages were required, up to 15 V, which may not be permitted in vivo. More recently, reduced GO was also exploited by Mac Kenna et al.,[57] who prepared an electroconductive hydrogel system comprising Jeffamine polyetheramine and poly(ethylene glycol) diglycidyl ether (PEGDGE). Thus, our material represents a novel and electrostimulated drug delivery system, particularly suitable for drugs characterized by an electronic structure capable of interacting with the surface of graphite and based, for the first time, on a thermoplastic biocompatible and bioabsorbable polymer, that is, PLLA, and on graphite. The possibility to produce a conductive composite containing graphite represents an important advantage with respect to the exploitation of GO or reduced GO, as the latter nanoparticles, because of the conversion of the planar sp^2 lattice into a sp^3 lattice, are characterized by a drastic reduction of electron mobility. Moreover, as shown in Figure 7e, another characteristic which makes our developed system extremely promising is related to its dimensional stability after the electrostimulation, a feature which is not always obtainable with other polymer systems, such as hydrogels. It is worth underlining that the film did not change its dimensions also in the saline solution at least for one month.

CONCLUSIONS

This study dealt with the application of PLLA-based composite films, which were made conductive by dispersing graphite into the polymer matrix, as electrostimulated drug delivery systems. The characterization of the prepared films demonstrated our preliminary hypothesis that from one part, graphite nanoplatelets allows to improve the material features, such as thermal, mechanical, and electrical properties, and from the other, promotes the homogeneous dispersion of the drug in the polymer film. Indeed, this study was based on the application of a porphyrin as drug model molecule, whose interactions with the surface of the filler were also found to improve, in turn, the dispersion/exfoliation of graphite nanoplatelets in the system.

The proper dispersion of high-aspect-ratio nanoplatelets corresponds to the formation of an electrically percolating network, resulting in a high electrical conductivity of the composite. This represent a significant advantage compared to the use of the most common applied graphite oxide, whose exploitation typically leads to an insufficient electrical conductivity.

Furthermore, it was demonstrated that the porphyrin release can be viably improved/tuned through the application of an electrical voltage to the composite film. That is, thanks to the exploitation of the synergy between graphite and a π-stacking-forming-molecule, such as porphyrin, we were able to develop, for the first time, an electrically controlled release system based on PLLA. Given the biocompatible (other than easily processable) nature of this latter, we believe our new concept system to open up many possibilities especially in the field of drug delivery.

ASSOCIATED CONTENT

Supporting Information

The Supporting Information is available free of charge on the ACS Publications website at DOI: 10.1021/acsami.6b08808.

FE-SEM micrograph of graphite nanoplatelets (A12 from Graphene Supermarket), 5,10,15,20-tetrakis(4-hydroxyphenyl)porphyrin (THPP) and FE-SEM micrograph of PLLA_G (PDF)

AUTHOR INFORMATION

Corresponding Author

*Tel +39 010 3536176; fax +39 010 3538733; e-mail orietta.monticelli@unige.it (O.M.).

Notes

The authors declare no competing financial interest.

ACKNOWLEDGMENTS

Mr. F. Franchini at Politecnico di Torino, Miss V. Ceresi, and Mr. A. Caviglione at Genova University are gratefully acknowledged for their precious help in the material characterization. Part of the activity by Alberto Fina in this in this work has received funding from the European Research Council (ERC) under the European Union's Horizon 2020 research

DOI: 10.1021/acsami.6b08808
ACS Appl. Mater. Interfaces 2016, 8, 24909−24917

and innovation programme grant agreement 639495-IN-THERM-ERC-2014-STG.

REFERENCES

(1) Chee, W. K.; Lim, H. N.; Huang, N. M.; Harrison, I. Nanocomposites of Graphene/Polymers: a Review. *RSC Adv.* **2015**, *5*, 68014−68051.
(2) Sengupta, R.; Bhattacharya, M.; Bandyopadhyay, S.; Bhowmick, A. K. A Review on the Mechanical and Electrical Properties of Graphite and Modified Graphite Reinforced Polymer composites. *Prog. Polym. Sci.* **2011**, *36*, 638−670.
(3) Wei, J.; Vo, T.; Inam, F. Epoxy/Graphene Nanocomposites − Processing and Properties: a Review. *RSC Adv.* **2015**, *5*, 73510−73524.
(4) Chakraborty, I.; Bodurtha, K. J.; Heeder, N. J.; Godfrin, M. P.; Tripathi, A.; Hurt, R. H.; Shukla, A.; Bose, A. Massive Electrical Conductivity Enhancement of Multilayer Graphene/Polystyrene Composites Using a Nonconductive Filler. *ACS Appl. Mater. Interfaces* **2014**, *6*, 16472−16475.
(5) Zhou, S.; Xu, J.; Yang, Q.-H.; Chiang, S.; Li, B.; Du, H.; Xu, C.; Kang, F. Experiments and Modeling of Thermal Conductivity of Flake Graphite/Polymer Composites Affected by Adding Carbon-based Nano-fillers. *Carbon* **2013**, *57*, 452−459.
(6) Wang, Y.; Polavarapu, L.; Liz-Marzan, L. M. Reduced Graphene Oxide-Supported Gold Nanostars for Improved SERS Sensing and Drug Delivery. *ACS Appl. Mater. Interfaces* **2014**, *6*, 21798−21805.
(7) Mendes, R. G.; Bachmatiuk, A.; Büchner, B.; Cuniberti, G.; Rümmeli, M. H. Carbon Nanostructures as Multi-functional Drug Delivery Platforms. *J. Mater. Chem. B* **2013**, *1*, 401−428.
(8) Jin, R.; Ji, X.; Yang, Y.; Wang, H.; Cao, A. Self-Assembled Graphene−Dextran Nanohybrid for Killing Drug Resistant Cancer Cells. *ACS Appl. Mater. Interfaces* **2013**, *5*, 7181−7189.
(9) Liu, Z.; Robinson, J. T.; Sun, X. M.; Dai, H. J. PEGylated Nanographene Oxide for Delivery of Water-Insoluble Cancer Drugs. *J. Am. Chem. Soc.* **2008**, *130*, 10876−10877.
(10) Tran, T. H.; Nguyen, H. T.; Pham, T. T.; Choi, J. Y.; Choi, H.-G.; Yong, C. S.; Kim, J. O. Development of a Graphene Oxide Nanocarrier for Dual-Drug Chemo-phototherapy to Overcome Drug Resistance in Cancer. *ACS Appl. Mater. Interfaces* **2015**, *7*, 28647−28655.
(11) Wang, C.; Ravi, S.; Garapati, U. S.; Das, M.; Howell, M.; Mallela, J.; Alwarappan, S.; Mohapatra, S. S.; Mohapatra, S. Multifunctional Chitosan Magnetic-Graphene (CMG) Nanoparticles: a Theranostic Platform for Tumortargeted co-Delivery of Drugs, Genes and MRI Contrast Agents. S. *J. Mater. Chem. B* **2013**, *1*, 4396−4405.
(12) Luo, Y.; Cai, X.; Li, H.; Lin, Y.; Du, D. Hyaluronic Acid-Modified Multifunctional Q-Graphene for Targeted Killing of Drug-Resistant Lung Cancer Cells. *ACS Appl. Mater. Interfaces* **2016**, *8*, 4048−4055.
(13) Feng, L.; Zhang, S.; Liu, Z. Graphene Based Gene Transfection. *Nanoscale* **2011**, *3*, 1252−1257.
(14) Kong, Z.; Zheng, W.; Wang, Q.; Wang, H.; Xi, F.; Liang, L.; Shen, J.-W. Charge-Tunable Absorption Behavior of DNA on Graphene. *J. Mater. Chem. B* **2015**, *3*, 4814−4820.
(15) Chen, B. A.; Liu, M.; Zhang, L. M.; Huang, J.; Yao, J. L.; Zhang, Z. J. Polyethylenimine-Functionalized Graphene Oxide as an Efficient Gene Delivery Vector. *J. Mater. Chem.* **2011**, *21*, 7736−7741.
(16) Xu, C.; Huang, Y.; Wu, J.; Tang, L.; Hong, Y. Triggerable Degradation of Polyurethanes for Tissue Engineering Applications. *ACS Appl. Mater. Interfaces* **2015**, *7*, 20377−20388.
(17) Ghasemi-Mobarakeh, L.; Prabhakaran, M. P.; Morshed, M.; Nasr-Esfahani, M. H.; Baharvand, H.; Kiani, S.; Al-Deyab, S. S.; Ramakrishna, S. Application of Conductive Polymers, Scaffolds and Electrical Stimulation for Nerve Tissue Engineering. *J. Tissue Eng. Regener. Med.* **2011**, *5*, e17−35.
(18) Ferraz, N.; Strømme, M.; Fellstrom, B.; Pradhan, S.; Nyholm, L.; Mihranyan, A. In Vitro and in Vivo Toxicity of Rinsed and Aged Nanocellulose−Polypyrrole Composites. *J. Biomed. Mater. Res., Part A* **2012**, *100*, 2128−2138.
(19) Humpolicek, P.; Kasparkova, V.; Saha, P.; Stejskal, J. Biocompatibility of Polyaniline. *Synth. Met.* **2012**, *162*, 722−727.
(20) Peramo, A.; Urbanchek, M. G.; Spanninga, S. A.; Povlich, L. K.; Cederna, P.; Martin, D. C. In Situ Polymerization of a Conductive Polymer in Acellular Muscle Tissue Constructs. *Tissue Eng., Part A* **2008**, *14*, 423−432.
(21) Balint, R.; Cassidy, N. J.; Cartmell, S. H. Conductive Polymers: Towards a Smart Biomaterial for Tissue Engineering. *Acta Biomater.* **2014**, *10*, 2341−2353.
(22) Wu, D.; Cheng, Y.; Feng, S.; Yao, Z.; Zhang, M. Crystallization Behavior of Polylactide/Graphene Composites. *Ind. Eng. Chem. Res.* **2013**, *52*, 6731−6739.
(23) Gardella, L.; Furfaro, D.; Galimberti, M.; Monticelli, O. On the Development of a Facile Approach Based on the Use of Ionic Liquids: Preparation of PLLA (sc-PLA)/High Surface Area Nano-graphite Systems. *Green Chem.* **2015**, *17*, 4082−4088.
(24) Wang, H. S.; Qiu, Z. B. Crystallization Kinetics and Morphology of Biodegradable Poly(l-lactic acid)/Graphene Oxide Nanocomposites: Influences of Graphene Oxide Loading and Crystallization Temperature. *Thermochim. Acta* **2012**, *527*, 40−46.
(25) Pinto, A. M.; Cabral, J.; Pacheco Tanaka, D. A.; Mendes, A. M.; Magalhães, F. D. Effect of Incorporation of Graphene Oxide and Graphene Nanoplatelets on Mechanical and Gas Permeability Properties of Poly(lactic acid) Films. *Polym. Int.* **2013**, *62*, 33−40.
(26) Li, X.; Xiao, Y.; Bergeret, A.; Longerey, M.; Che, J. Preparation of Polylactide/Graphene Composites from Liquid-Phase Exfoliated Graphite Sheets. *Polym. Compos.* **2014**, *35*, 396−403.
(27) Zhang, L.; Li, Y.; Wang, H.; Qiao, Y.; Chen, J.; Cao, S. Strong and Ductile Poly(lactic acid) Nanocomposite Films Reinforced with Alkylated Graphene Nanosheets. *Chem. Eng. J.* **2015**, *264*, 538−546.
(28) Forouharshad, M.; Gardella, L.; Furfaro, D.; Galimberti, M.; Monticelli, O. A Low-Environmental-Impact Approach for Novel Biocomposites Based on PLLA/PCL Blends and High Surface Area Graphite. *Eur. Polym. J.* **2015**, *70*, 28−36.
(29) Huang, X.; Qi, X.; Boey, F.; Zhang, H. Graphene-based Composites. *Chem. Soc. Rev.* **2012**, *41*, 666−686.
(30) Shen, Y.; Jing, T.; Ren, W.; Zhang, J.; Jiang, Z.-G.; Yu, Z.-Z.; Dasari, A. Chemical and Thermal Reduction of Graphene Oxide and its Electrically Conductive Polylactic Acid Nanocomposites. *Compos. Sci. Technol.* **2012**, *72*, 1430−1435.
(31) Bourlinos, A. B.; Georgakilas, V.; Zboril, R.; Steriotis, T. A.; Stubos, A. K. Liquid-Phase Exfoliation of Graphite Towards Solubilized Graphenes. *Small* **2009**, *5*, 1841−1845.
(32) Lotya, M.; Hernandez, Y.; King, P. J.; Smith, R. J.; Nicolosi, V.; Karlsson, L. S.; Blighe, F. M.; De, S.; Wang, Z. M.; McGovern, I. T.; Duesberg, G. S.; Coleman, J. N. Liquid Phase Production of Graphene by Exfoliation of Graphite in Surfactant/Water Solutions. *J. Am. Chem. Soc.* **2009**, *131*, 3611−3620.
(33) Ciesielski, A.; Samorì, P. Graphene *via* Sonication Assisted Liquid-Phase Exfoliation. *Chem. Soc. Rev.* **2014**, *43*, 381−398.
(34) Parviz, D.; Das, S.; Ahmed, H. S. T.; Irin, F.; Bhattacharia, S.; Green, M. J. Dispersions of Non-Covalently Functionalized Graphene with Minimal Stabilizer. *ACS Nano* **2012**, *6*, 8857−8867.
(35) Otsuki, J.; Nagamine, E.; Kondo, T.; Iwasaki, K.; Asakawa, M.; Miyake, K. Surface Patterning with Two-Dimensional Porphyrin Supramolecular Arrays. *J. Am. Chem. Soc.* **2005**, *127*, 10400.
(36) Geng, J.; Kong, B.-S.; Bo Yanga, S.; Jung, H.-T. Preparation of Graphene Relying on Porphyrin Exfoliation of Graphite. *Chem. Commun.* **2010**, *46*, 5091−5093.
(37) Hasobe, T.; Imahori, H.; Kamat, P. V.; Ahn, T. K.; Kim, S. K.; Kim, D.; Fujimoto, A.; Hirakawa, T.; Fukuzumi, S. Photovoltaic Cells Using Composite Nanoclusters of Porphyrins and Fullerenes with Gold Nanoparticles. *J. Am. Chem. Soc.* **2005**, *127*, 1216−1228.
(38) Geng, J.; Ko, Y. K.; Youn, S. C.; Kim, Y.-H.; Kim, S.-A.; Jung, D.-H.; Jung, H.-T. Synthesis of SWNT Rings by Noncovalent Hybridization of Porphyrins and Single-Walled Carbon Nanotubes. *J. Phys. Chem. C* **2008**, *112*, 12264.
(39) Cannon, J. B. Pharmaceutics and Drug Delivery Aspects of Heme and Porphyrin Therapy. *J. Pharm. Sci.* **1993**, *82*, 435−446.

DOI: 10.1021/acsami.6b08808
ACS Appl. Mater. Interfaces 2016, 8, 24909−24917

(40) Prasanth, C. S.; Karunakaran, S. C.; Paul, A. K.; Kussovski, V.; Mantareva, V.; Ramaiah, D.; Selvaraj, L.; Angelov, I.; Avramov, L.; Nandakumar, K.; Subhash, N. Antimicrobial Photodynamic Efficiency of Novel Cationic Porphyrins towards Periodontal Gram-positive and Gram-negative Pathogenic Bacteria. *Photochem. Photobiol.* **2014**, *90*, 628−640.
(41) Stojiljkovic, I.; Evavold, B. D.; Kumar, V. Antimicrobial Properties of Porphyrins. *Expert Opin. Invest. Drugs* **2001**, *10*, 309−320.
(42) Wikene, K. O.; Bruzell, E.; Tønnesen, H. H. Improved Antibacterial Phototoxicity of a Neutral Porphyrin in Natural Deep Eutectic Solvents. *J. Photochem. Photobiol., B* **2015**, *148*, 188−196.
(43) Hernandez, Y.; Nicolosi, V.; Lotya, M.; Blighe, F. M.; Sun, Z.; De, S.; Mcgovern, I. T.; Holland, B.; Byrne, M.; Gun'ko, Y. K.; Boland, J. J.; Niraj, P.; Duesberg, G.; Krishnamurthy, S.; Goodhue, R.; Hutchison, J.; Scardaci, V.; Ferrari, A. C.; Coleman, J. N. High-yield Production of Graphene by Liquid-phase Exfoliation of Graphite. *Nat. Nanotechnol.* **2008**, *3*, 563−568.
(44) Monticelli, O.; Bocchini, S.; Gardella, L.; Cavallo, D.; Cebe, P.; Germelli, G. Impact of Synthetic Talc on PLLA Electrospun Fibers. *Eur. Polym. J.* **2013**, *49*, 2572.
(45) Xu, J.-Z.; Chen, T.; Yang, C.-L.; Li, Z.-M.; Mao, Y.-M.; Zeng, B.-Q.; Hsiao, B. S. Isothermal Crystallization of Poly(L-lactide) Induced by Graphene Nanosheets and Carbon Nanotubes: a Comparative Study. *Macromolecules* **2010**, *43*, 5000−5008.
(46) Sun, Y.; He, C. B. Synthesis and Stereocomplex Crystallization of Poly(lactide)−Graphene Oxide Nanocomposites. *ACS Macro Lett.* **2012**, *1*, 709−713.
(47) Wang, H. S.; Qiu, Z. B. Crystallization Behaviors of Biodegradable Poly(l-lactic acid)/Graphene Oxide Nanocomposites from the Amorphous State. *Thermochim. Acta* **2011**, *526*, 229.
(48) Monticelli, O.; Putti, M.; Gardella, L.; Cavallo, D.; Basso, A.; Prato, M.; Nitti, S. New Stereocomplex PLA-Based Fibers: Effect of POSS on Polymer Functionalization and Properties. *Macromolecules* **2014**, *47*, 4718−4727.
(49) Shen, Y.; Jing, T.; Ren, W.; Zhang, J.; Jiang, Z.-G.; Yu, Z.-Z.; Dasari, A. Chemical and Thermal Reduction of Graphene Oxide and its Electrically Conductive Polylactic Acid Nanocomposites. *Compos. Sci. Technol.* **2012**, *72*, 1430−1435.
(50) Kim, I. H.; Jeong, Y. G. Polylactide/exfoliated Graphite Nanocomposites with Enhanced Thermal Stability, Mechanical Modulus, and Electrical Conductivity. *J. Polym. Sci., Part B: Polym. Phys.* **2010**, *48*, 850−858.
(51) Yu, J.; Wang, N.; Ma, X. Fabrication and Characterization of Poly(lactic acid)/Acetyl Tributyl Citrate/Carbon Black as Conductive Polymer Composites. *Biomacromolecules* **2008**, *9*, 1050−1057.
(52) Monticelli, O.; Calabrese, M.; Gardella, L.; Fina, A.; Gioffredi, E. Silsesquioxanes: Novel Compatibilizing Agents for Tuning the Microstructure and Properties of PLA/PCL Immiscible Blends. *Eur. Polym. J.* **2014**, *58*, 69−78.
(53) Murariu, M.; Dechief, A. L.; Bonnaud, L.; Paint, Y.; Gallos, A.; Fontaine, G.; Bourbigot, S.; Dubois, P. The production and properties of polylactide composites filled with expanded graphite. *Polym. Degrad. Stab.* **2010**, *95*, 889−900.
(54) Pinto, A. M.; Moreira, S.; Gonçalves, I. C.; Gama, F. M.; Mendes, A. M.; Magalhães, F. D. Biocompatibility of Poly(lactic acid) with Incorporated Graphene-based Materials. *Colloids Surf., B* **2013**, *104*, 229−238.
(55) Liu, H.-W.; Hu, S.-H.; Chen, Y.-W.; Chen, S.-Y. Characterization and Drug Release Behavior of Highly Responsive Chip-like Electrically Modulated Reduced Graphene Oxide−Poly(vinyl alcohol) Membranes. *J. Mater. Chem.* **2012**, *22*, 17311−17320.
(56) Servant, A.; Leon, V.; Jasim, D.; Methven, L.; Limousin, P.; Fernandez-Pacheco, E. V.; Prato, M.; Kostarelos, K. Graphene-based Electroresponsive Scaffolds as Polymeric Implants for On-Demand Drug Delivery. *Adv. Healthcare Mater.* **2014**, *3*, 1334−1343.
(57) Mac Kenna, N.; Calvert, P.; Morrin, A.; Wallace, G. G.; Moulton, S. E. Electro-stimulated Release from a Reduced Graphene Oxide Composite Hydrogel. *J. Mater. Chem. B* **2015**, *3*, 2530−2537.

DOI: 10.1021/acsami.6b08808
ACS Appl. Mater. Interfaces 2016, 8, 24909−24917